

Analysis of $\Lambda_c(2595)$, $\Lambda_c(2625)$, $\Lambda_b(5912)$, $\Lambda_b(5920)$ based on a chiral partner structure

Yohei Kawakami* and Masayasu Harada†

Department of Physics, Nagoya University, Nagoya, 464-8602, Jpana

(Dated: February 18, 2022)

We construct an effective hadronic model including $\Lambda_c(2595)$, $\Lambda_c(2625)$, $\Lambda_b(5912)$ and $\Lambda_b(5920)$ regarding them as chiral partners to $\Sigma_c(2455)$, $\Sigma_c(2520)$, Σ_b and Σ_b^* , respectively, with respecting the chiral symmetry and heavy-quark spin-flavor symmetry. We determine the model parameters from the experimental data for relevant masses and decay widths of $\Sigma_c^{(*)}$ and $\Lambda_c(2595)$. Then, we study the decay widths of $\Lambda_c(2625)$, $\Lambda_b(5912)$ and $\Lambda_b(5920)$. We find that, although the decay of $\Lambda_c(2595)$ is dominated by the resonant contribution through $\Sigma_c(2455)$, non-resonant contributions are important for $\Lambda_c(2625)$, $\Lambda_b(5912)$ and $\Lambda_b(5920)$, which reflects the chiral partner structure. We also study the radiative decays of the baryons, and show that each of their widths is determined from the radiative decay width of their chiral partners.

I. INTRODUCTION

Chiral symmetry and its spontaneous breaking is one of the most important properties to understand the structures of hadrons including light quarks. The spontaneous chiral symmetry breaking is expected to generate a part of hadron masses and causes mass difference between chiral partners. We expect that the study of chiral partner structure will provide a clue for understanding the chiral symmetry.

In Refs. [1–4], the chiral partner structure of heavy-light mesons was studied regarding the mesons with $J^P = (0^+, 1^+)$ such as (D_0^*, D_1) as the chiral partners to the mesons with $J^P = (0^-, 1^-)$ such as (D, D^*) based on the chiral symmetry combined with the heavy quark spin symmetry. In Refs. [5–7], doubly heavy baryons with negative parity were studied by regarding them as chiral partners to the positive parity heavy baryons. In these analysis, the heavy quark flavor symmetry in addition to the chiral symmetry and the heavy quark spin symmetry plays a very important role to relate the charm baryons to the bottom baryons. In Refs. [8, 9], chiral partner structure of heavy baryons including a charm quark is within the bound state approach based on the Skyrms model. In Ref. [10], the chiral partner structure of single heavy baryons was studied, in which the chiral partner of Σ_c baryon with positive parity is regarded as the Σ_c baryons with negative parity.

In the present work, we would like to propose a new possibility of the chiral partner structure for single heavy baryons differently from the one in Ref. [10], in which the chiral partners of Σ_Q ($Q = c, b$) baryons with positive parity are considered as Λ_Q baryons with negative parity: we regard $(\Lambda_c(2595; J^P = 1/2^-), \Lambda_c(2625; 3/2^-))$ as the chiral partners to $(\Sigma_c(2455; 1/2^+), \Sigma_c(2520; 3/2^+))$, and $(\Lambda_b(5912; 1/2^-), \Lambda_b(5920; 3/2^-))$ to $(\Sigma_b(1/2^+), \Sigma_b^*(3/2^+))$. Based on this chiral partner structure, we construct an effective model respecting

the chiral symmetry and the heavy-quark spin-flavor symmetry. Determining model parameters from the experimental data for relevant masses and decay widths of $\Sigma_c(2455)$, $\Sigma_c^*(2520)$ and $\Lambda_c(2595)$, we study the decay widths of $\Lambda_c^*(2625)$, $\Lambda_b(5912)$ and $\Lambda_b(5920)$.

This paper is organized as follows: In section II, we study the chiral structure of single heavy baryons (SHBs). We construct an effective Lagrangian in section III. Sections IV and V are devoted to study the masses and the hadronic decays of SHBs. We also study the radiative decays of SHBs in section VI. Finally, we give a summary and discussions in section VII.

II. CHIRAL STRUCTURE OF SINGLE HEAVY BARYONS

In this section, we study the chiral structure of single heavy baryons using interpolating quark fields.

First we consider interpolating field operators made from up or down quarks:

$$q_{L,R}^i, \quad (i = u, d), \quad (1)$$

where L and R denote left-handed and right-handed chirality, respectively. By using these, we can construct two combinations of diquarks carrying spin-zero which are expressed as

$$(q_L^i)^T C q_L^j, \quad (q_R^i)^T C q_R^j, \quad (2)$$

where T denote the transposition in the spinor space and $C = i\gamma^0\gamma^2$ is the charge conjugation matrix. When the relative angular momentum between two quarks are even, the indices i and j should be anti-symmetrized due to the Fermi statistics. In such a case, we can easily see that both of the above diquarks are chiral singlet. For clarifying this chiral structure, we introduce the following two diquarks which are chiral singlet:

$$\epsilon_{ij} (q_L^i)^T C q_L^j, \quad \epsilon_{ij} (q_R^i)^T C q_R^j, \quad (3)$$

where ϵ^{ij} is anti-symmetric tensor, $\epsilon_{ij} = -\epsilon_{ji}$, with $\epsilon_{ud} = 1$, and the summations over repeated indices are

* kawakami@hken.phys.nagoya-u.ac.jp

† harada@hken.phys.nagoya-u.ac.jp

understood. Since both of the above two diquarks are chiral singlet, two combination of them, which are parity eigenstates, are separately chiral singlet.

Now, let us introduce a field for the chiral-singlet light-quark cloud with $J^P = 0^+$ as

$$\Phi_{(+)} = \epsilon_{ij} (q_L^i)^T C q_L^j + \epsilon_{ij} (q_R^i)^T C q_R^j, \quad (4)$$

which belongs to $(1, 1)$ representation under $(\text{SU}(2)_L, \text{SU}(2)_R)$ symmetry. We construct a single heavy baryon by combining this light-quark cloud ($J^P = 0^+$) to a heavy quark Q ($Q = c, b$). The resultant baryon is a heavy-quark spin singlet, so that we identify it with the lightest Λ_Q ($Q = c, b$):

$$\Lambda_Q \sim Q \Phi_{(+)}, \quad \Lambda_Q = (\Lambda_c^+, \Lambda_b^0), \quad (5)$$

which belongs to $(1, 1)$ representation under $(\text{SU}(2)_L, \text{SU}(2)_R)$ symmetry.

Next, we consider the following diquark:

$$[\Phi^\mu]^{ij} = [q_L^T C \gamma^\mu q_R]^{ij} = (q_L^i)^T C \gamma^\mu q_R^j, \quad (6)$$

which belongs to $(2, 2)$ representation under $(\text{SU}(2)_L, \text{SU}(2)_R)$ symmetry. We can easily see that the following property is satisfied:

$$[q_R^T C \gamma^\mu q_L]^{ij} = -[q_L^T C \gamma^\mu q_R]^{ji}. \quad (7)$$

From these diquarks, we make two combinations of parity eigenstates:

$$\begin{aligned} [q_L^T C \gamma^\mu q_R]^{ij} + [q_R^T C \gamma^\mu q_L]^{ij} &= [q^T C \gamma^\mu q]^{ij} = [\Phi_{(3)}^\mu]^{ij}, \\ [q_L^T C \gamma^\mu q_R]^{ij} - [q_R^T C \gamma^\mu q_L]^{ij} &= [q^T C \gamma^\mu \gamma_5 q]^{ij} = [\Phi_{(1)}^\mu]^{ij}. \end{aligned} \quad (8)$$

From the property in Eq. (7), one can easily check that the indices of the diquark with $J^P = 1^+$ is symmetric in the light-quark flavor space, and those of the one with $J^P = 1^-$ is anti-symmetric, i.e.

$$\begin{aligned} [\Phi_{(3)}^\mu]^{ij} &= [\Phi_{(3)}^\mu]^{ji}, \\ [\Phi_{(1)}^\mu]^{ij} &= -[\Phi_{(1)}^\mu]^{ji}. \end{aligned} \quad (9)$$

From this we can easily see that, when the chiral symmetry is spontaneously broken into the isospin symmetry, $\Phi_{(3)}^\mu$ is the iso-triplet diquark with $J^P = 1^+$, and $\Phi_{(1)}^\mu$ is the iso-singlet diquark with $J^P = 1^-$.

The diquark Φ^μ combined with a heavy quark makes a set of heavy-quark doublets of single heavy baryons (SHBs) with $1/2^-$ and $3/2^-$ as

$$S_Q^\mu \sim Q \Phi^\mu, \quad (10)$$

where S_Q^μ denotes the field for the set of SHBs. The S_Q^μ includes iso-triplet SHBs and iso-singlet SHBs as

$$\begin{aligned} (\Sigma_Q^a(1/2^+), \Sigma_Q^{*a}(3/2^+)) &\sim Q \Phi_{(3)}^\mu, \\ (\Lambda_{Q1}(1/2^-), \Lambda_{Q1}^*(3/2^-)) &\sim Q \Phi_{(1)}^\mu, \end{aligned} \quad (11)$$

where we omitted the index μ in the left hand sides. It should be stressed that, since both $\Phi_{(3)}^\mu$ and $\Phi_{(1)}^\mu$ are included in one chiral multiplet Φ^μ , the heavy quark multiplet of $(\Lambda_{Q1}(1/2^-), \Lambda_{Q1}^*(3/2^-))$ is the chiral partner to that of $(\Sigma_Q(1/2^+), \Sigma_Q^*(3/2^+))$. In the present work, we identify $(\Sigma_Q(1/2^+), \Sigma_Q^*(3/2^+))$ with the lightest iso-triplet single-heavy baryons with positive parity, and $(\Lambda_{Q1}(1/2^-), \Lambda_{Q1}^*(3/2^-))$ with the lightest iso-singlet ones with negative parity:

$$\begin{aligned} (\Sigma_c, \Sigma_c^*) &= (\Sigma_c(2455; 1/2^+), \Sigma_c(2520; 3/2^+)), \\ (\Lambda_{c1}, \Lambda_{c1}^*) &= (\Lambda_c(2595; 1/2^-), \Lambda_c(2625; 3/2^-)), \\ (\Sigma_b, \Sigma_b^*) &= (\Sigma_b(1/2^+), \Sigma_b^*(3/2^+)), \\ (\Lambda_{b1}, \Lambda_{b1}^*) &= (\Lambda_b(5912; 1/2^-), \Lambda_b(5920; 3/2^-)). \end{aligned} \quad (12)$$

III. EFFECTIVE LAGRANGIAN

In this section we construct an effective Lagrangian for the relevant single heavy baryons (SHBs) based on the heavy-quark spin-flavor symmetry and the chiral symmetry. We use the field Λ_Q for expressing the SHBs belonging to the chiral singlet in Eq. (5). For expressing the SHBs belonging to chiral $(2, 2)$ representations we introduce the field S_Q^μ in Eq. (10) which transforms as

$$S_Q^\mu \xrightarrow{\text{Ch.}} g_R S_Q^\mu g_L^T, \quad (Q = c, b). \quad (13)$$

As we discussed in the previous section, we assume that the fields include the iso-triplet SHBs with positive parity and the iso-singlet SHBs with negative parity as chiral partners to each others. They are embedded into the field S_Q^μ as

$$S_Q^\mu = \hat{\Sigma}_Q^\mu + \hat{\Lambda}_{Q1}^\mu, \quad (14)$$

where $\hat{\Sigma}_Q^\mu$ and $\hat{\Lambda}_{Q1}^\mu$ include the iso-triplet and iso-singlet fields, respectively as

$$\hat{\Sigma}_Q^\mu = \begin{pmatrix} \Sigma_Q^{I=1\mu} & \frac{1}{\sqrt{2}} \Sigma_Q^{I=0\mu} \\ \frac{1}{\sqrt{2}} \Sigma_Q^{I=0\mu} & \Sigma_Q^{I=-1\mu} \end{pmatrix}, \quad (15)$$

$$\hat{\Lambda}_{Q1}^\mu = \begin{pmatrix} 0 & \frac{1}{\sqrt{2}} \Lambda_{Q1}^\mu \\ -\frac{1}{\sqrt{2}} \Lambda_{Q1}^\mu & 0 \end{pmatrix}. \quad (16)$$

These Σ_Q^μ and Λ_{Q1}^μ are decomposed into spin-3/2 baryon fields and spin-1/2 fields as

$$\Sigma_Q^\mu = \Sigma_Q^{*\mu} - \frac{1}{\sqrt{3}}(\gamma^\mu + v^\mu)\gamma_5 \Sigma_Q, \quad (17)$$

$$\Lambda_{Q1}^\mu = \Lambda_{Q1}^{*\mu} - \frac{1}{\sqrt{3}}(\gamma^\mu + v^\mu)\gamma_5 \Lambda_{Q1}, \quad (18)$$

where $\Sigma_Q^{*\mu}$ and $\Lambda_{Q1}^{*\mu}$ denote the spin-3/2 baryon fields, and Σ_Q and Λ_{Q1} the spin-1/2 fields, respectively. We

note that the parity transformation of the S_Q^μ field is given by

$$S_Q^\mu \xrightarrow{P} -\gamma^0 S_{Q\mu}^T, \quad (19)$$

where T denotes the transposition of the 2×2 matrix in the light-quark flavor space, and that the Dirac conjugate is defined as

$$\bar{S}_Q^\mu = S_Q^{\mu\dagger} \gamma^0. \quad (20)$$

We introduce a 2×2 matrix field M for scalar and pseudoscalar mesons including a light quark and a light anti-quark, which belongs to the $(2, 2)$ representation under the chiral $SU(2)_L \times SU(2)_R$ symmetry. The transformation properties of M under the chiral symmetry and the parity are given by

$$M \xrightarrow{\text{Ch.}} g_L M g_R^\dagger, \quad (21)$$

$$M \xrightarrow{P} M^\dagger. \quad (22)$$

We assume that the effective Lagrangian terms for M are constructed in such a way that the M has a vacuum expectation value (VEV) which breaks the chiral symmetry

spontaneously, and the VEV is proportional to the pion decay constant f_π ¹:

$$\langle M \rangle = \frac{f_\pi}{\sqrt{2}} \begin{pmatrix} 1 & 0 \\ 0 & 1 \end{pmatrix}. \quad (23)$$

In the following, for studying the decays of the single heavy baryons with emitting pions, we parameterize the field M as

$$M = f_\pi U, \quad (24)$$

where

$$U = e^{\frac{2i\pi}{f_\pi}}, \quad (25)$$

with π being the 2×2 matrix field including pions as

$$\pi = \frac{1}{2} \begin{pmatrix} \pi^0 & \sqrt{2}\pi^+ \\ \sqrt{2}\pi^- & -\pi^0 \end{pmatrix}. \quad (26)$$

Now, let us write down an effective Lagrangian including the baryon fields Λ_Q and S_Q^μ together with the meson field M , based on the heavy-quark spin-flavor symmetry and the chiral symmetry. We do not include the terms including more than square of M field or more than two derivatives. A possible Lagrangian is given by

$$\begin{aligned} \mathcal{L}_Q = & -\text{tr} \bar{S}_Q^\mu (v \cdot iD - \Delta_Q) S_{Q\mu} + \bar{\Lambda}_Q (v \cdot iD) \Lambda_Q \\ & + \frac{g_1}{2f_\pi} \text{tr} \left(\bar{S}_Q^\mu M^\dagger M S_{Q\mu} + \bar{S}_{Q\mu}^T M M^\dagger S_Q^{\mu T} \right) \\ & - \frac{g_2}{2f_\pi} \text{tr} \bar{S}_Q^\mu M^\dagger S_{Q\mu}^T M^T - \frac{g_2^v}{2m_{\Lambda_Q}} \text{tr} \bar{S}_Q^\mu M^\dagger S_{Q\mu}^T M^T \\ & - i \frac{h_1^I - i h_1^R}{4f_\pi^2} \text{tr} \left(\bar{S}_Q^\mu M^\dagger v \cdot \partial M S_{Q\mu} + \bar{S}_Q^{\mu T} M v \cdot \partial M^\dagger S_{Q\mu}^T \right) \\ & - i \frac{-h_1^I - i h_1^R}{4f_\pi^2} \text{tr} \left(\bar{S}_Q^\mu v \cdot \partial M^\dagger M S_{Q\mu} + \bar{S}_Q^{\mu T} v \cdot \partial M M^\dagger S_{Q\mu}^T \right) \\ & + \frac{h_2}{2f_\pi^2} \text{tr} \left(\bar{S}_Q^\mu v \cdot \partial M^\dagger S_{Q\mu}^T M^T + \bar{S}_Q^{\mu T} v \cdot \partial M S_{Q\mu} M^* \right) \\ & - \frac{g_3}{2\sqrt{2}f_\pi} \bar{\Lambda}_Q \text{tr} \left(\partial^\mu M S_{Q\mu} \tau^2 - \partial_\mu M^\dagger S_Q^{\mu T} \tau^2 \right) + \text{h.c.}, \end{aligned} \quad (27)$$

where m_{Λ_Q} ($Q = c, b$) are the masses of $\Lambda_c(2286)$ and Λ_b in the ground state, Δ_Q provides the difference between the chiral invariant masses of (Σ_Q, Λ_{Q1}) chiral multiplet and the chiral singlet Λ_Q with heavy-quark flavor violation included. g_i ($i = 1, 2, 3$), g_2^v , h_1^I , h_1^R and h_2 are dimensionless coupling constants. Note that we included g_2^v -term to incorporate the heavy-flavor violation needed for explaining the mass differences of charm and bottom sectors. Although we can add heavy-quark flavor violation terms corresponding to g_1 -term, such contributions are absorbed into the definition of Δ_Q . We expect that heavy-quark flavor violating corrections to other terms are small.

IV. MASSES AND $\Sigma_Q^{(*)} \rightarrow \Lambda_Q \pi$ DECAYS

In this section, we determine the coupling constants g_2 and g_2^v from masses of relevant heavy baryons, and g_3

¹ Here we adopt the normalization of $f_\pi = 92.4 \text{ MeV}$.

from $\Sigma_c^{(*)} \rightarrow \Lambda_c \pi$ decays. Then we make predictions of $\Sigma_b^{(*)} \rightarrow \Lambda_b \pi$ decays.

When the chiral symmetry is spontaneously broken, the light meson field M acquires its vacuum expectation value as in Eq. (23). Then the masses of $\Sigma_Q^{(*)}$ and $\Lambda_Q^{(*)}$ are expressed as

$$m(\Sigma_Q^{(*)}) = m_{\Lambda_Q} + \Delta_Q + g_1 f_\pi - \frac{g_2^Q}{2} f_\pi, \quad (28)$$

$$m(\Lambda_Q^{(*)}) = m_{\Lambda_Q} + \Delta_Q + g_1 f_\pi + \frac{g_2^Q}{2} f_\pi, \quad (29)$$

where g_2^Q is

$$g_2^Q = g_2 + g_2^v \frac{f_\pi}{m_{\Lambda_Q}}. \quad (30)$$

In the present analysis, we assume that the heavy-quark multiplet of $(\Lambda_{c1}, \Lambda_{c1}^*) = (\Lambda_c(2595; J^P = 1/2^-), \Lambda_c(2625; 3/2^-))$ is the chiral partner to the multiplet of $(\Sigma_c, \Sigma_c^*) = (\Sigma_c(2455; 1/2^+), \Sigma_c(2520; 3/2^+))$, and that $(\Lambda_{b1}, \Lambda_{b1}^*) = (\Lambda_b(5912; 1/2^-), \Lambda_b(5920; 3/2^-))$ to $(\Sigma_b, \Sigma_b^*) = (\Sigma_b(1/2^+), \Sigma_b(3/2^+))$. We list experimental data of their masses and full decay widths in Table I.

TABLE I. Experimental data of masses and decay widths of heavy baryons included in the present analysis

particle	J^P	mass[MeV]	full width[MeV]
Λ_c	$1/2^+$	2286.46 ± 0.14	no strong decays
$\Sigma_c^{++}(2455)$	$1/2^+$	2453.97 ± 0.14	$1.89_{-0.18}^{+0.09}$
$\Sigma_c^+(2455)$	$1/2^+$	2452.9 ± 0.4	< 4.6
$\Sigma_c^0(2455)$	$1/2^+$	2453.75 ± 0.14	$1.83_{-0.19}^{+0.11}$
$\Sigma_c^{++}(2520)$	$3/2^+$	$2518.41_{-0.19}^{+0.21}$	$14.78_{-0.40}^{+0.30}$
$\Sigma_c^+(2520)$	$3/2^+$	2517.5 ± 1.3	< 17
$\Sigma_c^0(2520)$	$3/2^+$	2518.48 ± 0.20	$15.3_{-0.5}^{+0.4}$
$\Lambda_c(2595)$	$1/2^-$	2595.25 ± 0.28	$2.59 \pm 0.30 \pm 0.47$
$\Lambda_c(2625)$	$3/2^-$	2628.11 ± 0.19	< 0.97
Λ_b	$1/2^+$	5619.58 ± 0.17	no strong decays
Σ_b^+	$1/2^+$	$5811.3_{-0.8}^{+0.9} \pm 1.7$	$9.7_{-2.8}^{+3.8} \pm 1.2$
Σ_b^0	$1/2^+$	-	-
Σ_b^-	$1/2^+$	$5815.5_{-0.5}^{+0.6} \pm 1.7$	$4.9_{-2.1}^{+3.1} \pm 1.1$
Σ_b^{++}	$3/2^+$	$5832.1 \pm 0.7 \pm 1.7$	$11.5_{-2.2}^{+2.7} \pm 1.0$
Σ_b^{*0}	$3/2^+$	-	-
Σ_b^{*-}	$3/2^+$	$5835.1 \pm 0.6 \pm 1.7$	$7.5_{-1.8}^{+2.2} \pm 0.9$
$\Lambda_b(5912)$	$1/2^-$	$5912.18 \pm 0.13 \pm 0.17$	< 0.66
$\Lambda_b(5920)$	$3/2^-$	5919.90 ± 0.19	< 0.63

We determine the values of the coupling constants g_2^Q ($Q = c, b$) from the mass differences ΔM_Q of chiral partners in the following way: First, we separately evaluate the mass differences of chiral partners with spin-1/2 and

spin-3/2 as

$$\begin{aligned} \Delta M_Q^{(1/2, \text{exp})} &= M_{\Lambda_{Q1}} - M_{\Sigma_Q}, \\ \Delta M_Q^{(3/2, \text{exp})} &= M_{\Lambda_{Q1}^*} - M_{\Sigma_Q^*}, \quad (Q = c, b), \end{aligned} \quad (31)$$

where $M_{\Lambda_{Q1}^{(*)}}$ and $M_{\Sigma_Q^{(*)}}$ are given by taking the isospin average of relevant masses. Using the values listed in Table I, we obtain

$$\frac{\Delta M_c^{(1/2, \text{exp})}}{f_\pi} = 1.19, \quad (32)$$

$$\frac{\Delta M_c^{(3/2, \text{exp})}}{f_\pi} = 1.53 \quad (33)$$

for charm sector. By taking the spin average of these values, we determine the center value of g_2^c as

$$g_2^c = \frac{1}{3} \left(\frac{\Delta M_c^{(1/2, \text{exp})}}{f_\pi} + 2 \frac{\Delta M_c^{(3/2, \text{exp})}}{f_\pi} \right) = 1.30. \quad (34)$$

By taking the violation of heavy-spin symmetry, we evaluate the error as

$$g_2^c = 1.30_{-|1.19-1.30|}^{+|1.53-1.30|} = 1.30_{-0.11}^{+0.23}. \quad (35)$$

Similarly, g_2^b is evaluated as

$$g_2^b = 0.980_{-0.046}^{+0.090}. \quad (36)$$

Let us determine the value of the coupling constant g_3 from $\Sigma_c \rightarrow \Lambda_c \pi$ decays. We use the experimental values of the full widths of $\Sigma_c^{++}(2455; 1/2^+)$, $\Sigma_c^0(2455; 1/2^+)$, $\Sigma_c^{++}(2520; 3/2^+)$ and $\Sigma_c^{*0}(2520; 3/2^+)$ with assuming that the one-pion decay is dominant decay mode for each particle. We first calculate four values of the effective couplings $g_3(\Sigma_c^{(*)++} \rightarrow \Lambda_c^{(*)+} \pi^+)$ and $g_3(\Sigma_c^{(*)0} \rightarrow \Lambda_c^{(*)+} \pi^-)$ from the corresponding decay widths. Then, taking the iso-spin average for $J^P = 1/2^+$ and $3/2^+$ separately, we obtain

$$\begin{aligned} g_3^{(1/2)} &= \frac{g_3(\Sigma_c^{++} \rightarrow \Lambda_c^+ \pi^+) + g_3(\Sigma_c^0 \rightarrow \Lambda_c^+ \pi^-)}{2} = 0.673, \\ g_3^{(3/2)} &= \frac{g_3(\Sigma_c^{*++} \rightarrow \Lambda_c^+ \pi^+) + g_3(\Sigma_c^{*0} \rightarrow \Lambda_c^+ \pi^-)}{2} = 0.695. \end{aligned} \quad (37)$$

The spin average of the above values are calculated as

$$g_3 = \frac{1}{3} \left(g_3^{(1/2)} + 2g_3^{(3/2)} \right) = 0.688. \quad (38)$$

We include the systematic error of the spin average and the statistical error of the experimental data as

$$g_3 = \left| g_3^{3/2} - g_3 \right|_{\text{stat.e.}} + \left| g_3^{1/2} - g_3 \right|_{\text{stat.e.}}, \quad (39)$$

to obtain

$$g_3 = 0.688_{-0.025}^{+0.013}. \quad (40)$$

TABLE II. Estimated values of the coupling constants g_2^Q and g_3 .

parameter	value
g_2^c	$1.30^{+0.23}_{-0.11}$
g_2^b	$0.980^{+0.090}_{-0.046}$
g_3	$0.688^{+0.013}_{-0.025}$

We summarize the estimated values of g_2^Q and g_3 in Table II. Using the estimated value of g_3 , we calculate the decay widths of $\Sigma_Q^{(*)} \rightarrow \Lambda_Q \pi$ as shown in Table III. This shows that the obtained widths of $\Sigma_c(J^P = 1/2^+)$

TABLE III. Decay widths $\Sigma_Q^{(*)} \rightarrow \Lambda_Q \pi$ calculated in our model. We use $\Sigma_c(2455)^{++} \rightarrow \Lambda_c^+ \pi^+$, $\Sigma_c(2455)^{++} \rightarrow \Lambda_c^+ \pi^+$, $\Sigma_c(2455)^{++} \rightarrow \Lambda_c^+ \pi^+$ and $\Sigma_c(2455)^{++} \rightarrow \Lambda_c^+ \pi^+$ to determine the coupling constant g_3 as explained in the text.

decay modes	our model [MeV]	expt. [MeV]
$\Sigma_c^{++} \rightarrow \Lambda_c^+ \pi^+$	$1.96^{+0.07}_{-0.14}$	$1.89^{+0.09}_{-0.18}$
$\Sigma_c^+ \rightarrow \Lambda_c^+ \pi^0$	$2.28^{+0.09}_{-0.17}$	< 4.6
$\Sigma_c^0 \rightarrow \Lambda_c^+ \pi^-$	$1.94^{+0.07}_{-0.14}$	$1.83^{+0.11}_{-0.19}$
$\Sigma_c^{*++} \rightarrow \Lambda_c^+ \pi^+$	$14.7^{+0.6}_{-1.1}$	$14.78^{+0.30}_{-0.40}$
$\Sigma_c^{*+} \rightarrow \Lambda_c^+ \pi^0$	$15.3^{+0.6}_{-1.1}$	< 17
$\Sigma_c^{*0} \rightarrow \Lambda_c^+ \pi^-$	$14.7^{+0.6}_{-1.1}$	$15.3^{+0.4}_{-0.5}$
$\Sigma_b^+ \rightarrow \Lambda_b^0 \pi^+$	$6.14^{+0.23}_{-0.45}$	$9.7^{+3.8}_{-2.8} {}^{+1.2}_{-1.1}$
$\Sigma_b^0 \rightarrow \Lambda_b^0 \pi^0$	$7.27^{+0.27}_{-0.53}$	-
$\Sigma_b^- \rightarrow \Lambda_b^0 \pi^-$	$7.02^{+0.27}_{-0.51}$	$4.9^{+3.1}_{-2.1} \pm 1.1$
$\Sigma_b^{*+} \rightarrow \Lambda_b^0 \pi^+$	$11.0^{+0.4}_{-0.8}$	$11.5^{+2.7}_{-2.2} {}^{+1.0}_{-1.5}$
$\Sigma_b^{*0} \rightarrow \Lambda_b^0 \pi^0$	$12.3^{+0.5}_{-0.9}$	-
$\Sigma_b^{*-} \rightarrow \Lambda_b^0 \pi^-$	$11.9^{+0.4}_{-0.9}$	$7.5^{+2.2}_{-1.8} {}^{+0.9}_{-1.4}$

and $\Sigma_c^*(3/2^+)$ are consistent with each other even though we used common coupling constant g_3 . This implies that heavy quark spin violation between them is small. Furthermore, the predicted widths of Σ_b and Σ_b^* obtained by the common g_3 coupling for charm and bottom sectors are consistent with experiments. This indicates that the violation of the heavy-quark flavor symmetry is small at this moment, but precise determination of them by future experiments might require the inclusion of heavy-quark flavor violation. We should note that the predicted

widths of $\Sigma_c^{(*)+} \rightarrow \Lambda_c^+ \pi^0$ are larger than those of their iso-spin partners since the phase space is larger due to the smallness of the mass of π^0 .

V. $\Lambda_{Q1}^{(*)} \rightarrow \Lambda_Q \pi \pi$ DECAYS

In this section, we consider $\Lambda_{Q1}^{(*)} \rightarrow \Lambda_Q \pi \pi$ decays. In Fig. 1, we plot the relevant diagrams for $\Lambda_{Q1}^{(*)} \rightarrow \Lambda_Q \pi^+ \pi^-$ in our model. In the diagrams (a), (b) and (d), $\Sigma_Q^{(*)}$ s

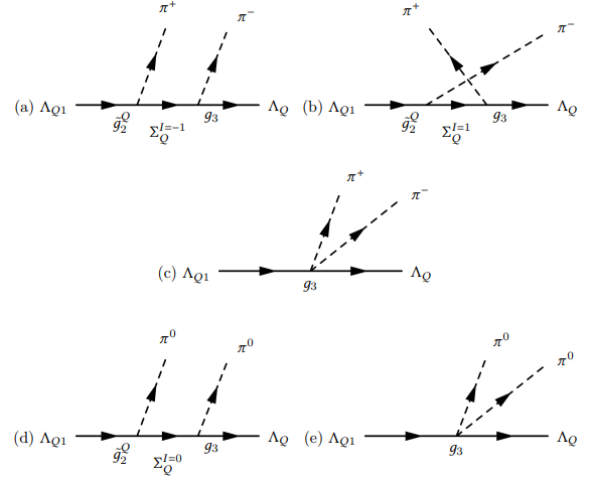


FIG. 1. Feynman diagrams contributing to $\Lambda_{Q1}^{(*)} \rightarrow \Lambda_Q \pi \pi$ decay. The effective coupling \tilde{g}_2^Q is defined as $\tilde{g}_2^Q = g_2^Q + (h_1^I + ih_2) \frac{E_\pi}{f_\pi}$, where E_π is the relevant pion energy. Similar Feynman diagrams contribute to $\Lambda_{Q1}^{(*)} \rightarrow \Lambda_Q \pi \pi$ decay.

appear as intermediate states, while in the diagram (c) and (e), $\Lambda_{Q1}^{(*)}$ and Λ_Q couple to two pions directly. It should be noticed that, due to the chiral partner structure, the coupling constant in (c) and (e) is equivalent to the $\Sigma_Q^{(*)} \rightarrow \Lambda_Q \pi$ coupling in (a), (b) and (d). Then, it is not suitable to drop the contributions in (c) and (e). Actually, as we will show below, They are not negligible for $\Lambda_{c1}^{(*)}$ and $\Lambda_{b1}^{(*)}$ decays.

From the diagrams in Fig. 1, the amplitude of $\Lambda_{Q1}^{(*)} \rightarrow \Lambda_Q \pi^+ \pi^-$ decays is calculated as

$$\begin{aligned}
 \mathcal{M} = & -\frac{g_3}{\sqrt{3}f_\pi} (p_2^\mu + p_3^\mu) \bar{u}(p_1, t) \left(\gamma_\mu + \frac{P_\mu}{M} \right) \gamma_5 u_1(P, s) \\
 & -\frac{g_3}{\sqrt{3}f_\pi} \left\{ g_2 + (h_1^I + ih_2) \frac{E_2(p_2)}{f_\pi} \right\} S_f^{++}(q) p_3^\mu \bar{u}(p_1, t) \left(\gamma_\mu + \frac{q_\mu}{m^{++}} \right) \gamma_5 (m^{++} + \not{q}) u_1(P, s) \\
 & -\frac{g_3}{\sqrt{3}f_\pi} \left\{ g_2 + (h_1^I + ih_2) \frac{E_3(p_3)}{f_\pi} \right\} S_f^0(k) p_2^\mu \bar{u}(p_1, t) \left(\gamma_\mu + \frac{k_\mu}{m^0} \right) \gamma_5 (m^0 + \not{k}) u_1(P, s), \quad (41)
 \end{aligned}$$

where P is the initial momentum of $\Lambda_{Q1}^{(*)}$, p_1 the momentum of Λ_Q , p_2 and p_3 are the momenta of pions, and k and q

the momenta of intermediate Σ_Q s. S_f is the propagator for the intermediate Σ_Q s given by

$$S_f(k) \equiv \frac{1}{m_{\Sigma_Q}^2 - k^2 + im_{\Sigma_Q}\Gamma_{\Sigma_Q}}, \quad (42)$$

where m_{Σ_Q} and Γ_{Σ_Q} are the mass and decay width of intermediate Σ_Q . We used isospin-averaged values of masses and decay widths in the present analysis. Similarly, the amplitude $\Lambda_{Q1} \rightarrow \Lambda_Q \pi^0 \pi^0$ decays is

$$\begin{aligned} \mathcal{M} = & -\frac{g_3}{\sqrt{3}f_\pi^2}(p_2^\mu + p_3^\mu)\bar{u}(p_1, t) \left(\gamma_\mu + \frac{P_\mu}{M} \right) \gamma_5 u_1(P, s) \\ & - \frac{g_3}{\sqrt{3}f_\pi} \left\{ g_2 + (h_1^I + ih_2) \frac{E_3(p_3)}{f_\pi} \right\} S_f^+(k) p_2^\mu \bar{u}(p_1, t) \left(\gamma_\mu + \frac{k_\mu}{m^+} \right) \gamma_5 (m^+ + \not{k}) u_1(P, s). \end{aligned} \quad (43)$$

We determine the relation between the values of h_1^I and h_2 from the full width of Λ_{c1} ($\Lambda_c(2595)$). Taking into account the errors of g_2^c , g_3 and the total width with Λ_{c1} , we determine the allowed range of h_1^I and h_2 as shown in Fig. 2. Using these values we calculate the two-pion

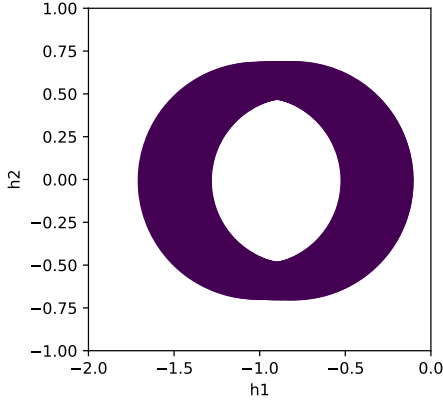


FIG. 2. Allowed range of h_1^I and h_2 shown by purple area.

decay widths of $\Lambda_c(2625)$, $\Lambda_b(5912)$ and $\Lambda_b(5920)$, which are summarized in Table IV.

TABLE IV. Predicted widths of $\Lambda_{Q1} \rightarrow \Lambda_Q \pi \pi$ decays.

initial	mode	Our model [MeV]	expt. [MeV]
$\Lambda_c(2595)$	$\Lambda_c \pi^+ \pi^-$	0.562-1.09	
	$\Lambda_c \pi^0 \pi^0$	1.23-2.31	
	sum	1.82-3.36 (input)	$2.59 \pm 0.30 \pm 0.47$
$\Lambda_c(2625)$	$\Lambda_c \pi^+ \pi^-$	0.0618-0.507	
	$\Lambda_c \pi^0 \pi^0$	0.0431-0.226	
	sum	0.106-0.733	< 0.97
$\Lambda_b(5912)$	$\Lambda_b \pi^+ \pi^-$	$(0.67-4.4) \times 10^{-3}$	
	$\Lambda_b \pi^0 \pi^0$	$(1.4-6.0) \times 10^{-3}$	
	sum	$(2.1-10) \times 10^{-3}$	< 0.66
$\Lambda_b(5920)$	$\Lambda_b \pi^+ \pi^-$	$(0.75-13) \times 10^{-3}$	
	$\Lambda_b \pi^0 \pi^0$	$(2.2-12) \times 10^{-3}$	
	sum	$(3.0-25) \times 10^{-3}$	< 0.63

The predicted decay width of $\Lambda_c(2625)$ is consistent with predictions of a quark model in Ref. [13]. We note that the predicted decay widths of $\Lambda_b(5912)$ and $\Lambda_b(5920)$ are extremely tiny due to the phase space suppression. As we will show in the next section, the radiative decay widths for $\Lambda_b(5912)$ and $\Lambda_b(5920)$ are comparable with or even larger than the hadronic decay widths.

Here we pick up several typical choices of h_1^I and h_2 , and study the contributions of the diagrams in Fig. 1 and their interferences. In Table V, we list four typical sets of h_1^I and h_2 together with the values of g_2^Q and g_3 .

TABLE V. Four typical parameter sets determined from $\Lambda_{c1} \rightarrow \Lambda_c \pi \pi$ decay width.

set	g_2^c	g_2^b	g_3	h_1^I	h_2
set 1	1.30	0.980	0.688	-0.277	0
set 2	1.30	0.980	0.688	-1.45	0
set 3	1.30	0.980	0.688	-0.450	0.500
set 4	1.30	0.980	0.688	-1.00	-0.500

Using four sets of parameters in Table V, we study contributions of intermediate states to $\Lambda_{Q1}^{(*)} \rightarrow \Lambda_Q \pi \pi$ decays,

which are shown in Tables VI-IX. Table VI shows the contributions of intermediate states to $\Lambda_c(2595; 1/2^-) \rightarrow \Lambda_c \pi \pi$

TABLE VI. Contributions of intermediate states to $\Lambda_c(2595; 1/2^-) \rightarrow \Lambda_c \pi \pi$ decay. “NR(c)” and “NR(e)” in the column for “intermediate states” indicate the non-resonant contributions expressed in Figs. 1(c) and 1(e), respectively. “ $\Sigma_c^0(a)$ ”, “ $\Sigma_c^{++}(b)$ ” and “ $\Sigma_c^+(d)$ ” indicate the resonant contributions in Figs. 1(a), 1(b) and 1(d), respectively. “ $\Sigma_c^{++}(b)$ & $\Sigma_c^0(a)$ ”, and so on indicate the contributions of the interferences.

decay mode	intermediate states	set 1 [keV]	set 2 [keV]	set 3 [keV]	set 4 [keV]
$\Lambda_c(2595; 1/2^-) \rightarrow \Lambda_c^+ \pi^+ \pi^-$	NR(c)	4.10	4.10	4.10	4.10
	$\Sigma_c^{++}(b)$	344	408	438	302
	$\Sigma_c^0(a)$	390	466	497	344
	$\Sigma_c^{++}(b)$ & $\Sigma_c^0(a)$	15.7	26.4	21.5	18.2
	NR(c) & $\Sigma_c^{++}(b)$	42.7	-49.1	36.3	-21.1
	NR(c) & $\Sigma_c^0(a)$	44.3	-51.5	38.1	-22.6
$\Lambda_c(2595; 1/2^-) \rightarrow \Lambda_c^+ \pi^0 \pi^0$	NR(e)	4.85	4.85	4.85	4.85
	$\Sigma_c^+(d)$	1.71×10^3	1.82×10^3	2.12×10^3	1.39×10^3
	NR(e) & $\Sigma_c^+(d)$	33.1	-41.6	63.7	-54.6
total		2.59×10^3	2.59×10^3	3.23×10^3	1.97×10^3

decay. More than half of this decay width is provided by the contribution in which Σ_c^+ exists as an intermediate state as in Fig. 1(d). This is because the threshold for $\Lambda_c(2595) \rightarrow \Sigma_c^+(2455) \pi^0$ decay is open. Accordingly, non-resonant (NR) contributions in Figs. 1(c) and (e) are very small. On the other hand, NR contributions to $\Lambda_c(2625)$, $\Lambda_b(5912)$

TABLE VII. Contributions of intermediate states to $\Lambda_c(2625; 3/2^-) \rightarrow \Lambda_c \pi \pi$ decay. “NR(c)” and “NR(e)” in the column for “intermediate states” indicate the non-resonant contributions expressed in Figs. 1(c) and 1(e), respectively. “ $\Sigma_c^{*0}(a)$ ”, “ $\Sigma_c^{*++}(b)$ ” and “ $\Sigma_c^{*+}(d)$ ” indicate the resonant contributions in Figs. 1(a), 1(b) and 1(d), respectively. “ $\Sigma_c^{*++}(b)$ & $\Sigma_c^{*0}(a)$ ”, and so on indicate the contributions of the interferences.

decay mode	intermediate states	set 1 [keV]	set 2 [keV]	set 3 [keV]	set 4 [keV]
$\Lambda_c(2625; 3/2^-) \rightarrow \Lambda_c^+ \pi^+ \pi^-$	NR(c)	58.4	58.4	58.4	58.4
	$\Sigma_c^{*++}(b)$	78.2	149	113	97.8
	$\Sigma_c^{*0}(a)$	76.7	157	114	102
	$\Sigma_c^{*++}(b)$ & $\Sigma_c^{*0}(a)$	7.44	22.0	12.5	13.6
	NR(c) & $\Sigma_c^{*++}(b)$	93.2	-135	74.8	-62.8
	NR(c) & $\Sigma_c^{*0}(a)$	92.3	-138	74.3	-65.3
$\Lambda_c(2625; 3/2^-) \rightarrow \Lambda_c^+ \pi^0 \pi^0$	NR(e)	43.0	43.0	43.0	43.0
	$\Sigma_c^{*+}(d)$	69.1	125	97.8	83.1
	NR(e) & $\Sigma_c^{*+}(d)$	73.2	-105	60.4	-50.1
total		591	177	648	219

and $\Lambda_b(5920)$ are comparable to resonant contributions, partly because the threshold for $\Sigma_Q \pi$ decays are not open. As we stressed, the coupling constant g_3 in Figs. 1(c) and (e) is fixed from $\Sigma_c \rightarrow \Lambda_c \pi$ decay based on the chiral partner structure. Then, the experimental check of non-resonant contributions will give a clue to the chiral symmetry structure.

VI. RADIATIVE DECAYS

In this section, we consider radiative decays of the heavy baryons. The relevant Lagrangian is given by

$$\begin{aligned}
\mathcal{L}_{\text{rad}} = & \frac{r_1}{F} \text{tr} \left(\bar{S}_Q^\mu Q_{\text{light}} S_Q^\nu + \bar{S}_Q^{\mu T} Q_{\text{light}} S_Q^{\nu T} \right) F_{\mu\nu} \\
& + \frac{r_2}{F} \text{tr} \left(\bar{S}_Q^\mu Q_{\text{light}} S_Q^\nu - \bar{S}_Q^{\mu T} Q_{\text{light}} S_Q^{\nu T} \right) \tilde{F}_{\mu\nu} \\
& + \frac{r_3}{F^2} \bar{\Lambda}_Q \text{tr} \left(S_Q^\mu \tau^2 M Q_{\text{light}} v^\nu - S_Q^{\mu T} \tau^2 M^\dagger Q_{\text{light}} v^\nu \right) F_{\mu\nu} \\
& + \text{h.c.} \\
& + \frac{r_4}{F^2} \bar{\Lambda}_Q \text{tr} \left(S_Q^\mu \tau^2 M Q_{\text{light}} v^\nu + S_Q^{\mu T} \tau^2 M^\dagger Q_{\text{light}} v^\nu \right) \tilde{F}_{\mu\nu} \\
& + \text{h.c.},
\end{aligned} \tag{44}$$

TABLE VIII. Contributions of intermediate states to $\Lambda_b(5912; 1/2^-) \rightarrow \Lambda_b \pi \pi$ decay. “NR(c)” and “NR(e)” in the column for “intermediate states” indicate the non-resonant contributions expressed in Figs. 1(c) and 1(e), respectively. “ $\Sigma_b^-(a)$ ”, “ $\Sigma_b^+(b)$ ” and “ $\Sigma_b^0(d)$ ” indicate the resonant contributions in Figs. 1(a), 1(b) and 1(d), respectively. “ $\Sigma_b^+(b)$ & $\Sigma_b^-(a)$ ”, and so on indicate the contributions of the interferences.

decay mode	intermediate states	set 1 [keV]	set 2 [keV]	set 3 [keV]	set 4 [keV]
$\Lambda_b(5912; 1/2^-) \rightarrow \Lambda_b^0 \pi^+ \pi^-$	NR(c)	0.61	0.61	0.61	0.61
	$\Sigma_b^+(b)$	0.42	2.3	0.95	1.3
	$\Sigma_b^-(a)$	0.35	1.9	0.80	1.1
	$\Sigma_b^+(b)$ & $\Sigma_b^-(a)$	0.018	0.11	0.043	0.062
	NR(c) & $\Sigma_b^+(b)$	0.71	-1.7	0.47	-0.87
	NR(c) & $\Sigma_b^-(a)$	0.65	-1.5	0.38	-0.75
$\Lambda_b(5912; 1/2^-) \rightarrow \Lambda_b^0 \pi^0 \pi^0$	NR(e)	1.40	1.40	1.40	1.40
	$\Sigma_b^0(d)$	0.97	5.0	2.1	2.9
	NR(e) & $\Sigma_b^0(d)$	1.6	-3.8	1.0	-1.9
total		6.8	4.3	7.8	3.9

TABLE IX. Contributions of intermediate states to $\Lambda_b(5920; 3/2^-) \rightarrow \Lambda_c \pi \pi$ decay. “NR(c)” and “NR(e)” in the column for “intermediate states” indicate the non-resonant contributions expressed in Figs. 1(c) and 1(e), respectively. “ $\Sigma_b^{*-}(a)$ ”, “ $\Sigma_b^{*+}(b)$ ” and “ $\Sigma_b^{*0}(d)$ ” indicate the resonant contributions in Figs. 1(a), 1(b) and 1(d), respectively. “ $\Sigma_b^{*+}(b)$ & $\Sigma_b^{*-}(a)$ ”, and so on indicate the contributions of the interferences.

decay mode	intermediate states	set 1 [keV]	set 2 [keV]	set 3 [keV]	set 4 [keV]
$\Lambda_b(5920; 3/2^-) \rightarrow \Lambda_b^0 \pi^+ \pi^-$	NR(c)	2.4	2.4	2.4	2.4
	$\Sigma_b^{*+}(b)$	0.87	5.2	2.1	3.0
	$\Sigma_b^{*-}(a)$	0.80	4.8	1.9	2.8
	$\Sigma_b^{*+}(b)$ & $\Sigma_b^{*-}(a)$	0.040	0.27	0.10	0.15
	NR(c) & $\Sigma_b^{*+}(b)$	2.1	-5.1	1.3	-2.6
	NR(c) & $\Sigma_b^{*-}(a)$	2.0	-4.9	1.1	-2.4
$\Lambda_b(5920; 3/2^-) \rightarrow \Lambda_b^0 \pi^0 \pi^0$	NR(e)	3.5	3.5	3.5	3.5
	$\Sigma_b^{*0}(d)$	1.3	7.3	3.0	4.2
	NR(e) & $\Sigma_b^{*0}(d)$	3.0	-7.2	1.9	-3.7
total		16	6.4	17	7.2

where $F_{\mu\nu}$ is the field strength of the photon and $\tilde{F}_{\mu\nu}$ is its dual tensor: $\tilde{F}_{\mu\nu} = (1/2)\epsilon_{\mu\nu\rho\sigma}F^{\rho\sigma}$. r_i ($i = 1, \dots, 4$) are dimensionless constants, and F is a constant with dimension one. In this analysis, we take $F = 350$ MeV following Ref. [11]. We note that the values of the constants r_i are of order one based on quark models [11].

Let us first study the electromagnetic intramultiplet transitions governed by the r_1 -term in Eq. (44). Let B^* denotes the decaying baryon with spin-3/2 ($B^* = \Lambda_{Q1}^*, \Sigma_Q^*$), and B the daughter baryon with spin-1/2 ($B = \Lambda_{Q1}, \Sigma_Q$). Then the radiative decay width is given by

$$\Gamma_{B^* \rightarrow B\gamma} = C_{B^*B\gamma}^2 \frac{16\alpha r_1^2}{9F^2} \frac{m_B}{m_{B^*}} E_\gamma^3 \quad (45)$$

where α is the electromagnetic fine structure constant, E_γ is the photon energy and $C_{B^*B\gamma}$ is the Clebsh-Gordon

constant given by

$$\begin{aligned} C_{\Sigma_c^{*++}\Sigma_c^{++}\gamma} &= C_{\Sigma_b^{*+}\Sigma_b^{+}\gamma} = \frac{2}{3}, \\ C_{\Sigma_c^{*+}\Sigma_c^{+}\gamma} &= C_{\Sigma_b^{*0}\Sigma_b^0\gamma} = \frac{1}{6}, \\ C_{\Sigma_c^{*0}\Sigma_c^0\gamma} &= C_{\Sigma_b^{*-}\Sigma_b^-\gamma} = -\frac{1}{3}, \\ C_{\Lambda_{c1}^{*+}\Lambda_{c1}^{+}\gamma} &= C_{\Lambda_b^{*0}\Lambda_b^0\gamma} = -\frac{1}{6}. \end{aligned} \quad (46)$$

From this, one naively expects that ratios of radiative decay widths are determined from the squares of these constants as

$$\begin{aligned} C_{\Sigma_c^{*++}\Sigma_c^{++}\gamma}^2 : C_{\Sigma_c^{*+}\Sigma_c^{+}\gamma}^2 : C_{\Sigma_c^{*0}\Sigma_c^0\gamma}^2 : C_{\Lambda_{c1}^{*+}\Lambda_{c1}^{+}\gamma}^2 \\ = 16 : 1 : 4 : 1. \end{aligned} \quad (47)$$

In Table X, we show our predictions on the decay widths of $\Lambda_{Q1}^* \rightarrow \Lambda_{Q1}\gamma$ and $\Sigma_Q^* \rightarrow \Sigma_Q\gamma$ comparing with the predictions in Refs. [16] and [15]. The predicted values for $\Sigma_Q^* \rightarrow \Sigma_Q\gamma$ decay widths are consistent with the ratio in Eq. (47), while the values for $\Lambda_{Q1}^* \rightarrow \Lambda_{Q1}\gamma$ decay

widths are much smaller than the ratio in Eq. (47). This is because the mass differences between Λ_{Q1}^* and Λ_{Q1} are quite small generating huge phase space suppression. We note that our predictions are consistent with the predictions in Refs. [16] and [15].

TABLE X. Radiative decay widths of $\Lambda_{Q1}^* \rightarrow \Lambda_{Q1}\gamma$ and $\Sigma_Q^* \rightarrow \Sigma_Q\gamma$ in unit of keV. The values in the row indicated by “Predictions” are our predicted values, where r_1 is an undetermined parameter of $\mathcal{O}(1)$. For comparison, we list predictions in Refs. [16] and [15].

decay mode	Predictions	[16]	[15]
	[keV]	[keV]	[keV]
$\Sigma_c^{*++} \rightarrow \Sigma_c^{++}\gamma$	$12 r_1^2$	11.6	-
$\Sigma_c^{*+} \rightarrow \Sigma_c^{+}\gamma$	$0.75 r_1^2$	0.85	-
$\Sigma_c^{*0} \rightarrow \Sigma_c^0\gamma$	$3.1 r_1^2$	2.92	-
$\Lambda_{c1}^{*+} \rightarrow \Lambda_{c1}^{+}\gamma$	$0.13 r_1^2$	-	$0.107 c_R^2$
$\Sigma_b^{*+} \rightarrow \Sigma_b^{+}\gamma$	$0.42 r_1^2$	0.60	-
$\Sigma_b^{*0} \rightarrow \Sigma_b^0\gamma$	$0.024 r_1^2$	0.02	-
$\Sigma_b^{*-} \rightarrow \Sigma_b^{-}\gamma$	$0.089 r_1^2$	0.06	-
$\Lambda_{b1}^{*0} \rightarrow \Lambda_{b1}^0\gamma$	$0.0013 r_1^2$	-	-

We next study the $\Lambda_{Q1}^{(*)} \rightarrow \Sigma_Q^{(*)}\gamma$ decays which concern the r_2 -term. The decay widths are expressed as

$$\begin{aligned}
\Gamma_{\Lambda_{Q1} \rightarrow \Sigma_Q \gamma} &= \frac{16\alpha r_2^2}{9F^2} \frac{m_{\Sigma_Q}}{m_{\Lambda_{Q1}}} E_\gamma^3, \\
\Gamma_{\Lambda_{Q1} \rightarrow \Sigma_Q^* \gamma} &= \frac{8\alpha r_2^2}{9F^2} \frac{m_{\Sigma_Q^*}}{m_{\Lambda_{Q1}}} E_\gamma^3, \\
\Gamma_{\Lambda_{Q1}^* \rightarrow \Sigma_Q \gamma} &= \frac{4r_2^2}{9F^2} \frac{m_{\Sigma_Q}}{m_{\Lambda_{Q1}^*}} E_\gamma^3, \\
\Gamma_{\Lambda_{Q1}^* \rightarrow \Sigma_Q^* \gamma} &= \frac{20\alpha r_2^2}{9F^2} \frac{m_{\Sigma_Q^*}}{m_{\Lambda_{Q1}^*}} E_\gamma^3.
\end{aligned} \tag{48}$$

In Table XI, we show our predictions comparing with those in Ref. [15].

TABLE XI. Radiative decay widths of $\Lambda_{Q1}^* \rightarrow \Sigma_Q^{(*)}\gamma$ in unit of keV. The values in the row indicated by “Predictions” are our predicted values, where r_2 is an undetermined parameter of $\mathcal{O}(1)$. For comparison, we list predictions in Ref. [15].

decay mode	Predictions	[15]
	[keV]	[keV]
$\Lambda_{c1}^+ \rightarrow \Sigma_c^{+}\gamma$	$250 r_2^2$	$127 c_{RS}^2$
$\Lambda_{c1}^+ \rightarrow \Sigma_c^{*+}\gamma$	$21 r_2^2$	$6 c_{RS}^2$
$\Lambda_{c1}^{*+} \rightarrow \Sigma_c^{+}\gamma$	$120 r_2^2$	$58 c_{RS}^2$
$\Lambda_{c1}^{*+} \rightarrow \Sigma_c^{*+}\gamma$	$160 r_2^2$	$54 c_{RS}^2$
$\Lambda_{b1}^0 \rightarrow \Sigma_b^0\gamma$	$98 r_2^2$	-
$\Lambda_{b1}^0 \rightarrow \Sigma_b^{*0}\gamma$	$25 r_2^2$	-
$\Lambda_{b1}^{*0} \rightarrow \Sigma_b^0\gamma$	$31 r_2^2$	-
$\Lambda_{b1}^{*0} \rightarrow \Sigma_b^{*0}\gamma$	$81 r_2^2$	-

The r_3 -term generates the $\Lambda_{Q1}^{(*)} \rightarrow \Lambda_Q\gamma$ decay, the

width of which is expressed as

$$\Gamma_{\Lambda_{Q1}^{(*)} \rightarrow \Lambda_Q \gamma} = \frac{8\alpha r_3^2 f_\pi^2}{27F^4} \frac{m_{\Lambda_Q}}{m_{\Lambda_{Q1}^{(*)}}} E_\gamma^3. \tag{49}$$

In Table XII, we show our predictions together with the ones in Ref. [15].

TABLE XII. Radiative decay widths of $\Lambda_{Q1}^* \rightarrow \Lambda_Q\gamma$ in unit of keV. The values in the row indicated by “Predictions” are our predicted values, where r_3 is an undetermined parameter of $\mathcal{O}(1)$. For comparison, we list predictions in Ref. [15].

decay mode	Predictions	[15]
	[keV]	[keV]
$\Lambda_{c1} \rightarrow \Lambda_c\gamma$	$25 r_3^2$	$191 c_{RT}^2$
$\Lambda_{c1}^* \rightarrow \Lambda_c\gamma$	$35 r_3^2$	$253 c_{RT}^2$
$\Lambda_{b1} \rightarrow \Lambda_b\gamma$	$27 r_3^2$	-
$\Lambda_{b1}^* \rightarrow \Lambda_b\gamma$	$29 r_3^2$	-

The width of $\Sigma_Q^{(*)} \rightarrow \Lambda_Q\gamma$ decay via the r_4 -term is given by

$$\Gamma_{\Sigma_Q^{(*)} \rightarrow \Lambda_Q \gamma} = \frac{8\alpha r_4^2 f_\pi^2}{3F^4} \frac{m_{\Lambda_Q}}{m_{\Sigma_Q^{(*)}}} E_\gamma^3, \tag{50}$$

and the predicted values are shown in Table XIII.

TABLE XIII. Radiative decay widths of $\Sigma_Q^* \rightarrow \Lambda_Q\gamma$ in unit of keV. The values in the row indicated by “Predictions” are our predicted values, where r_4 is an undetermined parameter of $\mathcal{O}(1)$. For comparison, we list predictions in Ref. [16].

decay mode	Predictions	[16]
	[keV]	[keV]
$\Sigma_c^+ \rightarrow \Lambda_c^{+}\gamma$	$43 r_4^2$	164
$\Sigma_c^{*+} \rightarrow \Lambda_c^{+}\gamma$	$110 r_4^2$	893
$\Sigma_b^0 \rightarrow \Lambda_b^0\gamma$	$74 r_4^2$	288
$\Sigma_b^{*0} \rightarrow \Lambda_b^0\gamma$	$99 r_4^2$	435

VII. A SUMMARY AND DISCUSSIONS

We constructed an effective hadronic model regarding $\Lambda_{Q1} = \{\Lambda_c(2595, J^P = 1/2^-), \Lambda_b(5912, 1/2^-)\}$ and $\Lambda_{Q1}^* = \{\Lambda_c^*(2625, 3/2^-), \Lambda_b^*(5920, 3/2^-)\}$ as chiral partners to $\Sigma_Q = \{\Sigma_c(2455, 1/2^+), \Sigma_b(1/2^+)\}$ and $\Sigma_Q^* = \{\Sigma_c^*(2520, 3/2^+), \Sigma_b^*(3/2^+)\}$, respectively, based on the chiral symmetry and heavy-quark spin-flavor symmetry. We determined the model parameters from the experimental data for relevant masses and decay widths of $\Sigma_c(2455, 1/2^+)$, $\Sigma_c^*(2520, 3/2^+)$ and $\Lambda_c(2595, 1/2^-)$. Then, we studied the decay widths of $\Lambda_c^*(2625)$, $\Lambda_b(5912)$ and $\Lambda_b^*(5920)$. We showed that the coupling constant for non-resonant contributions depicted in Figs. 1(c) and (e) is fixed from the $\Sigma_c^{(*)}$ decays reflecting the chiral partner

structure. As a result, the decay of $\Lambda_c(2595)$ is dominated by the resonant contribution through $\Sigma_c(2455)$ depicted in Fig. 1(d), since the threshold of $\Lambda_c(2595) \rightarrow \Sigma_c^+(2455)\pi^0$ decay is open. We found non-resonant contributions depicted in Figs. 1(c) and (e) are comparable to resonant contributions for $\Lambda_c(2625)$, $\Lambda_b(5912)$ and $\Lambda_b(5920)$, partly because the threshold for $\Sigma_Q\pi$ decays are not open. Our result indicates that studying non-resonant contributions will give a clue to understand the chiral partner structure for single heavy baryons.

We also studied the radiative decays of $\Sigma_Q^{(*)}$ and $\Lambda_{Q1}^{(*)}$ using effective interaction Lagrangians in Eq. (44). We showed that there is a relation among $\Sigma_Q^* \rightarrow \Sigma_Q\gamma$ and $\Lambda_{Q1}^* \rightarrow \Lambda_{Q1}\gamma$ decays reflecting the chiral partner structure, which can be checked in future experiments.

In Table XIV, we summarize our predictions of the decay widths of single heavy baryons. We expect that comparison of these predictions with experimental data will give some clues to understand the chiral structure of single heavy baryons. We note that, since the hadronic decays of $\Lambda_{b1}(5912)$ and $\Lambda_{b1}^*(5920)$ are suppressed by the small phase space factors, radiative decays may be dom-

inant modes.

Several comments are in order.

The present model does not include the decay $\Lambda_{Q1} \rightarrow \Lambda_Q\pi\pi$ via Σ_Q^* , which needs two pions in the D -wave in the heavy quark limit. We expect that such decays are suppressed compared with the decays having two pions in the S -wave. Similarly, we expect that the decay $\Lambda_{Q1}^* \rightarrow \Lambda_Q\pi\pi$ via Σ_Q is also suppressed.

It is interesting to extend the present model including only two flavors to the one with the strange quark in addition based on the chiral $SU(3)_L \times SU(3)_R$ symmetry. In the case, the flavor $\bar{3}$ representation including Λ_{Q1} becomes the chiral partner to the flavor 6 representation including Σ_Q . We leave the analysis in future publication.

Acknowledgments

This work was supported partly by JSPS KAKENHI Grant Number JP16K05345. We would like to thank Daiki Suenaga for useful discussions and comments.

-
- [1] M. A. Nowak, M. Rho and I. Zahed, Phys. Rev. D **48**, 4370 (1993) doi:10.1103/PhysRevD.48.4370 [hep-ph/9209272].
 - [2] W. A. Bardeen and C. T. Hill, Phys. Rev. D **49**, 409 (1994) doi:10.1103/PhysRevD.49.409 [hep-ph/9304265].
 - [3] W. A. Bardeen, E. J. Eichten and C. T. Hill, Phys. Rev. D **68**, 054024 (2003) doi:10.1103/PhysRevD.68.054024 [hep-ph/0305049].
 - [4] M. A. Nowak, M. Rho and I. Zahed, Acta Phys. Polon. B **35**, 2377 (2004) [hep-ph/0307102].
 - [5] Y. L. Ma and M. Harada, Phys. Lett. B **748**, 463 (2015) doi:10.1016/j.physletb.2015.07.046 [arXiv:1503.05373 [hep-ph]].
 - [6] Y. L. Ma and M. Harada, Phys. Lett. B **754**, 125 (2016) doi:10.1016/j.physletb.2016.01.011 [arXiv:1510.07481 [hep-ph]].
 - [7] Y. L. Ma and M. Harada, arXiv:1709.09746 [hep-ph].
 - [8] M. A. Nowak, M. Praszalowicz, M. Sadzikowski and J. Wasiluk, Phys. Rev. D **70**, 031503 (2004) doi:10.1103/PhysRevD.70.031503 [hep-ph/0403184].
 - [9] M. Harada and Y. L. Ma, Phys. Rev. D **87**, no. 5, 056007 (2013) doi:10.1103/PhysRevD.87.056007 [arXiv:1212.5079 [hep-ph]].
 - [10] Y. R. Liu and M. Oka, Phys. Rev. D **85**, 014015 (2012) doi:10.1103/PhysRevD.85.014015 [arXiv:1103.4624 [hep-ph]].
 - [11] M. A. Nowak and I. Zahed, Phys. Rev. D **48**, 356 (1993). doi:10.1103/PhysRevD.48.356
 - [12] H. Nagahiro, S. Yasui, A. Hosaka, M. Oka and H. Noumi, Phys. Rev. D **95**, no. 1, 014023 (2017) doi:10.1103/PhysRevD.95.014023 [arXiv:1609.01085 [hep-ph]].
 - [13] A. J. Arifi, H. Nagahiro and A. Hosaka, Phys. Rev. D **95**, no. 11, 114018 (2017) doi:10.1103/PhysRevD.95.114018 [arXiv:1704.00464 [hep-ph]].
 - [14] P. L. Cho, Phys. Lett. B **285**, 145 (1992)
 - [15] P. L. Cho, Phys. Rev. D **50**, 3295 (1994) doi:10.1103/PhysRevD.50.3295 [hep-ph/9401276].
 - [16] N. Jiang, X. L. Chen and S. L. Zhu, Phys. Rev. D **92**, no. 5, 054017 (2015) doi:10.1103/PhysRevD.92.054017 [arXiv:1505.02999 [hep-ph]].
 - [17] S. Scherer and M. R. Schindler, arXiv:hep-ph/0505265
 - [18] C. Vafa and E. Witten, Nucl. Phys. B **234**, 173 (1984)
 - [19] S. Coleman, J. Math. Phys. **7**, 787 (1966)
 - [20] J. Beringer *et al.* (Particle Data Group), Phys. Rev. D **86** 010001 (2012)
 - [21] C. Patrignani *et al.* (Particle Data Group), Chin. Phys. C **40**, 100001 (2016)
 - [22] N. Isgur and M. B. Wise, Phys. Lett. B **232**, 113 (1989)
 - [23] N. Isgur and M. B. Wise, Phys. Lett. B **237**, 527 (1990)
 - [24] A. F. Falk, Nucl. Phys. B **378** (1992) 79-94
 - [25] A. Hosaka, T. Hyodo, K. Sudoh, Y. Yamaguchi, and S. Yasui (2017), <http://dx.doi.org/10.1016/j.pnpnp.2017.04.003>.

TABLE XIV. Predicted decay widths of single heavy baryons (SHBs). The row indicated by “Our model” shows the predictions of the present analysis. The row indicated by “exp.” shows the experimental values for the full width of the relevant SHBs, in which “-” implies no experimental data.

SHB	J^P	decay modes	Our model [MeV]	exp. [MeV]
Σ_c^{++}	$1/2^+$	$\Lambda_c \pi^+$	$1.96^{+0.07}_{-0.14}$	$1.89^{+0.09}_{-0.18}$
Σ_c^+	$1/2^+$	$\Lambda_c \pi^0$	$2.28^{+0.09}_{-0.17}$	< 4.6
		$\Lambda_c \gamma$	$0.043 r_4^2$	
Σ_c^0	$1/2^+$	$\Lambda_c \pi^-$	$1.94^{+0.07}_{-0.14}$	$1.83^{+0.11}_{-0.19}$
Σ_c^{*++}	$3/2^+$	$\Lambda_c \pi^+$	$14.7^{+0.6}_{-1.1}$	$14.78^{+0.30}_{-0.40}$
		$\Sigma_c^{*+} \gamma$	$0.012 r_1^2$	
Σ_c^{*+}	$3/2^+$	$\Lambda_c \pi^0$	$15.3^{+0.6}_{-1.1}$	< 17
		$\Sigma_c^+ \gamma$	$0.75 r_1^2 \times 10^{-3}$	
		$\Lambda_c \gamma$	$0.11 r_4^2$	
Σ_c^{*0}	$3/2^+$	$\Lambda_c \pi^-$	$14.7^{+0.6}_{-1.1}$	$15.3^{+0.4}_{-0.5}$
		$\Sigma_c^0 \gamma$	$3.1 r_1^2 \times 10^{-3}$	
Λ_{c1}	$1/2^-$	$\Lambda_c \pi^+ \pi^-$	0.562-1.09	$2.59 \pm 0.30 \pm 0.47$
		$\Lambda_c \pi^0 \pi^0$	1.23-2.31	
		$\Sigma_c^+ \gamma$	$0.25 r_2^2$	
		$\Sigma_c^{*+} \gamma$	$0.021 r_2^2$	
		$\Lambda_c \gamma$	$0.025 r_3^2$	
Λ_{c1}^*	$3/2^-$	$\Lambda_c \pi^+ \pi^-$	0.0618-0.507	< 0.97
		$\Lambda_c \pi^0 \pi^0$	0.0431-0.226	
		$\Lambda_{c1} \gamma$	$0.13 r_1^2 \times 10^{-3}$	
		$\Sigma_c^+ \gamma$	$0.12 r_2^2$	
		$\Sigma_c^{*+} \gamma$	$0.16 r_2^2$	
		$\Lambda_c \gamma$	$0.035 r_3^2$	
Σ_b^+	$1/2^+$	$\Lambda_b \pi^+$	$6.14^{+0.23}_{-0.45}$	$9.7^{+3.8}_{-2.8} {}^{+1.2}_{-1.1}$
Σ_b^0	$1/2^+$	$\Lambda_b \pi^0$	$7.27^{+0.27}_{-0.53}$	-
		$\Lambda_b^0 \gamma$	$0.074 r_4^2$	
Σ_b^-	$1/2^+$	$\Lambda_b \pi^-$	$7.02^{+0.27}_{-0.51}$	$4.9^{+3.1}_{-2.1} \pm 1.1$
Σ_b^{*+}	$3/2^+$	$\Lambda_b^0 \pi^+$	$11.0^{+0.4}_{-0.8}$	$11.5^{+2.7}_{-2.2} {}^{+1.0}_{-1.5}$
		$\Sigma_b^+ \gamma$	$0.42 r_1^2 \times 10^{-3}$	
Σ_b^{*0}	$3/2^+$	$\Lambda_b \pi^0$	$12.3^{+0.5}_{-0.9}$	-
		$\Sigma_b^+ \gamma$	$0.024 r_1^2 \times 10^{-3}$	
		$\Lambda_b \gamma$	$0.074 r_4^2$	
Σ_b^{*-}	$3/2^+$	$\Lambda_b \pi^-$	$11.9^{+0.4}_{-0.9}$	$7.5^{+2.2}_{-1.8} {}^{+0.9}_{-1.4}$
		$\Sigma_b^- \gamma$	$0.089 r_1^2 \times 10^{-3}$	
		$\Lambda_b \gamma$	$0.099 r_4^2$	
Λ_{b1}	$1/2^-$	$\Lambda_b \pi^+ \pi^-$	$(0.67-4.4) \times 10^{-3}$	< 0.66
		$\Lambda_b \pi^0 \pi^0$	$(1.4-6.0) \times 10^{-3}$	
		$\Sigma_b^0 \gamma$	$0.098 r_2^2$	
		$\Sigma_b^{*0} \gamma$	$0.025 r_2^2$	
		$\Lambda_b \gamma$	$0.027 r_3^2$	
Λ_{b1}^*	$3/2^-$	$\Lambda_b \pi^+ \pi^-$	$(0.75-13) \times 10^{-3}$	< 0.63
		$\Lambda_b \pi^0 \pi^0$	$(2.2-12) \times 10^{-3}$	
		$\Lambda_{b1} \gamma$	$0.0013 r_1^2 \times 10^{-3}$	
		$\Sigma_b^0 \gamma$	$0.031 r_2^2$	
		$\Sigma_b^{*0} \gamma$	$0.081 r_2^2$	
		$\Lambda_b \gamma$	$0.029 r_3^2$	